

Characterizing the limits of 3-photon microscopy as a tool for deep imaging of whole, cortical bone tissue

Samantha Z. Bratcher¹, Nicole E. Chernavsky¹, Christopher B. Schaffer¹, Karl J. Lewis¹

¹Meinig School of Biomedical Engineering, Cornell University, Ithaca, NY
szb3@cornell.edu

INTRODUCTION: Osteocytes have emerged as the primary mechanosensors in bone with a rising need to study their mechanobiology within the context of their *in vivo* microenvironment. These cells form dense networks interconnected with slender canaliculi. However, many optical techniques struggle to penetrate the dense and highly scattering mineralization within bone. Two-photon (2P) microscopy can successfully observe osteocyte molecular signaling *in vivo* in the third metatarsal (MT3) of mice but remains limited by achievable imaging depth¹. Three-photon (3P) microscopy is a novel imaging platform that offers increased depth penetration over 2P fluorescence imaging. In addition, third harmonic generation (THG) reveals material interfaces without the need for exogenous labels, allowing for the visualization of the interface between the bone and lacuno-canalicular network (LCN) and potentially the LCN and the osteocyte. Wu and colleagues depicted some of 3P's capabilities, observing *in vivo* osteocytes and canaliculi within mouse calvaria as well as penetrating to depths that reach the marrow where bone lining cells were visible². Nonetheless, further characterization is needed to establish 3P imaging in long bones to assess maximal imaging penetration along with longer wavelength excitation. In this study, we hypothesized that 3P microscopy of *ex vivo* cortical bone will yield increased depth penetration and greater data variety compared to 2P in long bones.

METHODS: All procedures were approved by the Cornell University IACUC. 16–20-week-old mice expressing osteocyte-targeted DMP-1 CRE activated GCaMP6f, a fluorescent calcium indicator, were used^{3,4}. Bilateral third metatarsals (MT3s) and femurs were dissected and fixed for 24 hours in zinc formalin. Bones were then soaked overnight in 1mM CaCl₂ to maximize GCaMP6f fluorescence brightness. Samples were divided into two groups based on excitation wavelength: 2P excitation at 920 nm and 3P excitation at 1320 nm. Images were collected using a Monaco laser (Coherent) with a 25x water immersion objective (Olympus XLPLN25XWMP, NA=1.05) in ScanImage (MBF Bioscience). Power was exponentially adjusted through depth to optimally maintain signal intensity through bone depth. Z-stacks at 512x512 pixel resolution were taken at the diaphysis through the anterior-coronal plane, except for the tibia, which was imaged through the medial-sagittal plane. Data were imported into FIJI for quantification. A 200 μ m-wide rectangle was centered on the bone, and cells outside were excluded to avoid variations in fluorescence intensity caused by differences in depth due to the curved bone surface. Cells were then counted through the z-stack depth in the fluorescence channel using 3D segmentation, and their intensities normalized to background ROIs manually chosen every 10 slices. Further analysis of signal-to-noise ratio (SNR) was performed in MATLAB. Slices beyond the endocortical bone surface in the MT3 were not included in cell counting.

RESULTS: Second harmonic generation (SHG) returned the strongest signal in both 2P and 3P, brightly revealing the bone matrix with dark spots denoting osteocyte lacunae in preliminary results (Figure 1). Notably, THG produced during 3P resolves the very fine and narrow canaliculi of the LCN (Figure 1D). Surprisingly, bone marrow was visible as a weak fluorescent signal despite no exogenous labeling. This may be due to leakiness of DMP1 as a Cre expressor or autofluorescence. Qualitative differences in image quality appeared when comparing 2P and 3P stacks, most notable in the femur as an increase in image depth and overall brightness in 3P (Figure 2 A-B). Similar performance in capturing GCaMP fluorescent osteocytes within the MT3 was found using 2P and 3P, reaching the marrow space beyond 90 μ m (Figure 2C). The marrow space in the femur was not reached with either 2P or 3P; however, 3P maintained a stronger signal, capturing a greater quantity of cells at 10 μ m and beyond (Figure 2E). Interestingly, peak quantity of cells captured appeared at different depths between 2P and 3P, with 3P peak cell capture occurring at deeper slice. SNR was higher in 2P stacks than 3P in the MT3, with a stark increase with depth (Figure 2D). SNR remained initially higher in 2P than 3P in the femur, but dropped as depth increased, with 3P surpassing at depths beyond 50 μ m (Figure 2F).

DISCUSSION: Preliminary results suggest in the smaller metatarsal and at depths up to 50 μ m in larger bones 3P microscopy has comparable performance compared to 2P. The robust SNR and depth penetration from 2P is likely a function of available laser power with the physical components of the imaging system, which cannot be matched currently at 3P. SHG signal was comparable for 3P and 2P. An advantage of 3P imaging is the capability of THG imaging in addition to fluorescence and SHG imaging modalities, which together produce comprehensive images of both bone tissue and osteocytes from whole specimens without exogenous labeling and with enough resolution to distinguish canaliculi (Figure 1D). Three-P microscopy offers an exciting opportunity to multiplex cellular function, microarchitecture, and material organization in a single intravital imaging process. Future work to establish this intravital imaging approach will include analysis of tibiae and humeri, cell viability assays, evaluation of longer wavelength 3P imaging to achieve better depth penetration and SNR, and *in vivo* loading with simultaneous fluorescent imaging of calcium signaling events.

SIGNIFICANCE: Here we report the establishment of a new multiphoton imaging approach, three-photon microscopy, for studying embedded osteocytes in mouse long bones. The data here show superior fluorescent signal to noise ratio for 3P over 2P at depths over 50 μ m, and dye-free micromorphological resolution using THG.

REFERENCES: 1) Lewis+ (2017) *PNAS*; 2) Wu+ (2018) *Optics*; 3) Madisen+ (2015) *Neuron*; 4) Lu+ (2007) *J. Dental Res.*

IMAGES AND TABLES:

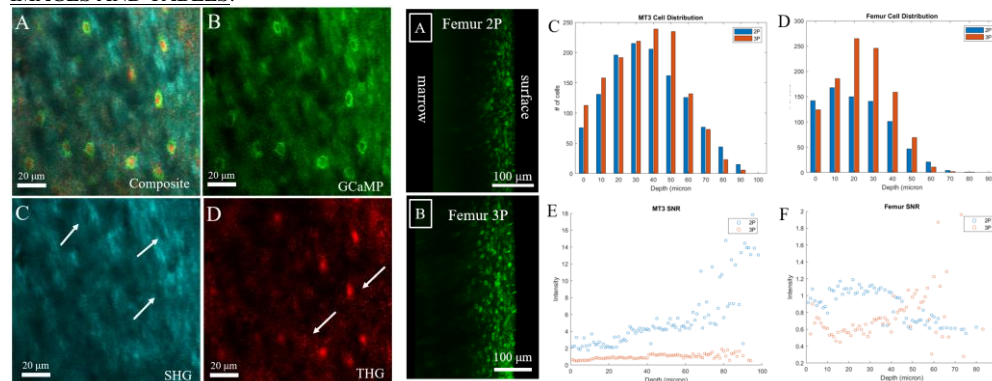


Figure 1. Zoomed image of femur cortical bone captured using 3P microscopy. (A) Composite image with each channel separated into (B) osteocyte bodies in GCaMP, (C) bone matrix in SHG, and (D) lacunae and canaliculi in THG. White arrows depict lacunae in SHG and

Figure 2. Representative 3D projection of a femur diaphysis turned to a side view with the surface on the right and the marrow space on the left. Images captured using (A) 2P and (B) 3P. Number of cells through z-stack depth were quantified using 3D segmentation in the (C) MT3 and (D) femur, with the femur showing a noticeably higher quantity of captured cells in 3P at depths beyond 50 μ m. SNR was then calculated through depth in (E) MT3 and (F) femur, with 3P showing a similar advantage over 2P beyond 50 μ m.